Office of Naval Research
Department of the Navy
Contract Nonr 220(43)

MEASUREMENTS OF THE WATER SURFACE CONTOUR BEHIND A HYDROFOIL OF MODERATE ASPECT RATIO

by

J. Brentjes

Hydrodynamics Laboratory
Kármán Laboratory of Fluid Mechanics and Jet Propulsion
California Institute of Technology
Pasadena, California

Report No. E-110.4 February 1964

Department of the Navy
Office of Naval Research
Contract Nonr 220(43)

MEASUREMENTS OF THE WATER SURFACE CONTOUR BEHIND A HYDROFOIL OF MODERATE ASPECT RATIO

by

J. Brentjes

Hydrodynamics Laboratory
Karman Laboratory of Fluid
Mechanics and Jet Propulsion
California Institute of Technology
Pasadena, California

Approved by A. J. Acosta
T. Y. Wu

Report No. E-110.4

February 1964

SUMMARY

An experimental program has been carried out for the measurement of the water surface contour due to a submerged hydrofoil of finite span. Because of the hydrofoil downwash, the water surface has a rather pronounced depression in the form of a long, narrow trough which extends many chords aft the hydrofoil. When the trailing vortex cores becomes sufficiently close to the water surface depression, flash ventilation of the vortices and the entire upper surface has been observed to occur abruptly.

The model used here was a hydrofoil with a NACA 16-206 section and a rectangular plan form, mounted on a NACA 16-006 strut. The hydrofoil has a chord of 3 inches and an aspect-ratio of 1.33. It has been found that the length and depth of the surface depression, and the location of the trough bottom are well defined functions of the Froude number and of the ratio of chord-to-submergence depth. It has also been observed that the distance between the trailing vortex core and the lowest points of the depression is an important parameter in effecting the onset of ventilating flow. This investigation covers a range of flow velocity, angle of attack, depth of submergence, and the flap angle deflection.

TABLE OF CONTENTS

Nomenclature

h	depth of submergence with respect to leading edge of the hydrofoil (ft.)
d'	maximum surface depression with respect to undisturbed surface (ft.)
L	lift force
ℓ	longitudinal or downstream distance from leading edge (ft.)
w	transverse distance from hydrofoil mid-span (ft.)
c	hydrofoil chord = 0.25 ft.
V	water velocity (fps)
$Fr = \frac{V}{\sqrt{gc}}$	Froude number based on chord
α	angle of attack (deg)
C_L	lift coefficient

1. Introduction

In the development of hydrofoil systems operating near the free water surface, it is important to determine the effects of the free surface on the basic characteristics of hydrofoil performance. Other than its effects on the lift, wave drag, moment of force of a hydrofoil, the free surface has an additional important effect on the change of the basic flow configuration by the inception of cavitation and ventilation about the hydrofoil. The formation of an air bubble by ventilation at the tips and upper surface of a submerged flat plate has been shown and discussed by Wadlin, Ramsen and Vaughan (1)*. It was reported that when the flow velocity past a hydrofoil, held at high angles of attack and submerged at shallow depths, is sufficiently large, air was observed to enter the trailing vortices from downstream. As the speed was increased the entrained air proceeded forward along a helical path inside the vortices until it reached the model, causing the entire upper side to be ventilated.

Similar observations have been made at this Hydrodynamics Laboratory using a hydrofoil with a NACA 16-206 section and a rectangular plan form. A 16mm motion picture (Ref. 2) presents some typical observations and experimental results, showing the effect of speed, angle of attack, operating depth and flap angles on the ventilation characteristics.

These experimental observations showed that due to the hydrofoil downwash, the water surface had a rather pronounced depression in the form of a long, narrow trough which extended many chords aft the hydrofoil, but before the well known wave pattern would be established further downstream. The results gave evidences that this water surface depression was very important to the initiation of ventilation. Apparently, this surface depression brings the free surface closer to the trailing vortices which represent a low pressure region (compared with

---

* Number in parenthesis indicate the references at the end of text.

the ambient) in the flow; hence air bubbles tend to migrate from the surface to the low pressure field of the tip vortices. When the depth of submergence was sufficiently small, and these vortex cores sufficiently close to the surface depression, flash ventilation of the vortices and the entire upper surface was observed to occur abruptly.

As was pointed out in Ref. (1) and later in (3), when the upper surface becomes ventilated, the lift of the hydrofoil suddenly drops by as much as 45 percent. This loss in lift and the large downstream disturbances produced by the trailing cavities are the important reasons for studying this phenomena from the standpoint of engineering application. The problem is also of interest in view of the determination of the critical conditions for ventilation inception and its bearing on related free-boundary flows. Consequently, it was decided to explore in a systematic manner the mechanism and conditions under which this type of ventilation takes place.

The first part of these studies involved the determination of the water surface contour behind a hydrofoil. Three important parameters --depth of submergence, velocity, angle of attack--were considered in this experimental program. Aspect ratio, though it can be important, was kept fixed in this study. Measurements were made of the surface contour, and in particular, the magnitude and location of the maximum surface depression were recorded for several velocities, angles of attack and foil depths.

2. Experimental Setup

The hydrofoil used in this experimental program was the NACA 16-206 section without flap. The chord of the hydrofoil was three inches and the span four inches; hence the aspect ratio was 4/3. There was no taper and the tips were square and parallel to each other. The foil was mounted at mid-span on a ten inch long strut which had a NACA 16-006 section profile and a chord of 2.25 inches. Table I shows the coordinates of the strut and foil.

The model was tested in the Free-Surface Water Tunnel which

has a test section 20 inches wide and eight feet long. The water depth under normal operating conditions is about 20 inches. Although it was recognized that the water surface contour could be a sensitive function of channel depth, width, and velocity, the effect of changes in channel geometry were not explored in these preliminary experiments. Figure 1 shows the apparatus used in this program. The model was supported from an elevating mechanism which permits the model to be positioned vertically with a repeatability of 0.001 feet. The water surface contour was determined with a depth gage which could be positioned at various distances behind and to the side of the model. The longitudinal distance, ℓ, was measured from the leading edge of the hydrofoil and the transverse distance, w, was measured from the centerline of the model. The reference level of the surface was taken to be the water surface in the absence of the model. This reference surface was determined with the depth gage for each run with a different velocity, since the water surface level is affected slightly by the tunnel speed. The reference depth of the foil was determined during each run by lowering the model to the water surface until the trailing edge just touched the water surface. A correction of $\Delta h = c \sin\alpha$, where c denotes the chord and α the angle of attack, was applied to account for the vertical distance between the leading and trailing edges of the hydrofoil. Thus the reference position of the hydrofoil depth is taken to be the distance from the leading edge to the undisturbed water surface at all times.

The water surface contour was measured for the velocity V equal to 10, 15, 20, and 24.5 feet per second, with angle of attack α held at 2, 4, and 8 degrees, and depth-to-chord ratio set at 1.0, 0.5, and 0.25. Figures 4 through 8 show the resulting contours to scale. The maximum water surface depression d', was investigated further for a large number of foil depths and also for -4 degrees angle of attack. These results are shown in Figs. 9 and 10. Figure 11 shows the relationship between water depth and Froude number and also the lift coefficient. This lift coefficient data was obtained from Ref. (3), which presents the results of a test program conducted with the present hydro-

foil in the Free-Surface Water Tunnel.

3. Discussion of Results

The effect of foil submergence on the extent of the water surface displacement is most significant. This effect is seen in the photographs of Fig. 3 and in the measured surface profiles of Fig. 4. This latter figure is drawn to scale for a velocity of 15 fps and 8° angle of attack. It shows how the water surface at the centerline gradually slopes downward to a point which is about eight chords aft the leading edge of the hydrofoil. At 15 fps, this is the observed position of the maximum surface depression for all depths of submergence tested with this hydrofoil model. Downstream of this location the surface rises up again and begins to form a "rooster tail" at the centerline. The graphs of Figs. 5 and 6 give further information on the effect of angle of attack and the Froude number on the surface contour. The transverse profiles in Fig. 7 show how the rooster tail downstream of the hydrofoil develops. The growth of the rooster tail along the centerline is particularly noticeable at a velocity of 10 fps and, as can be seen, it rises above the undisturbed water level. This same phenomenon also occurred at higher velocities, but it took place further downstream (at the entrance of the tunnel diffuser) where it could not be measured.

The effect of angle of attack on the water surface profile is illustrated in Fig. 5. Again the maximum depth of the surface depression occurred eight chord lengths aft of the leading edge. Thus it seems that the longitudinal location of the maximum surface depression depends only on the velocity or, rather, on the Froude number based on chord. It is interesting to note also that the rooster tail formed only at moderate and high angles of attack; for the angle of attack about 2 and 4 degrees, the water surface tended to smooth out very gradually far downstream.

Figure 6 shows the effect of velocity on the longitudinal surface depression for an angle of attack of 8°. At 24.5 feet per second the depth of the water trough became tremendous and extended very

far downstream. For these same conditions the transverse profiles are presented in Fig. 7. Note that the cross sections were taken at regular intervals from the foil leading edge. The star indicates the approximate location of maximum water depth, d'. Although the length and depth of the surface depression increased with velocity, the width of the trough at the surface as well as at its deepest point was smaller for the high velocities. This is an important result from the standpoint of incipient tip ventilation. As was discussed before, the ventilation was always triggered from this trough, and proceeded forward to the foil tips. When the low local pressure field in the tip vortices becomes so close to the water surface, a passage is formed for the air to enter the vortex. Hence if the distance from these tip vortices to the surface is sufficiently large, ventilation will not occur at all.

In order to determine the effect of model depth, and of angle of attack on the surface depression depth d' in greater detail, a large number of readings of d' were taken at small intervals of foil depth. The effect of the Froude number is shown in Fig. 9. The most interesting result here is that the surface depression did not occur when hydrofoil was right at the water surface, but rather when it was somewhat below the surface. In fact, with an increase in the Froude number, the submergence required for maximum surface depression increased also. It should be noted here that the reason for negative surface depression is the fact that the foil depth was measured with respect to the foil leading edge. Hence for the negative values of h/c the hydrofoil was planing.

The dashed line in this Fig. 9 marks the points at which the tip vortices began to ventilate. When the hydrofoil was raised from a deep submergence toward the free surface, the ventilated tip vortices formed at these points. The ventilation of the entire upper surface occurred after the maximum value of d' had been reached. This state of ventilation will be called superventilation. The hydrofoil depth at which this superventilation was initiated varied from test to test somewhat and the individual points are, therefore, not marked. There was a considerable hysteresis effect on tip ventilation and superventilation. When the hydro-

foil was lowered below the point of incipient ventilation, after having established ventilation, the cavity would remain for many seconds until all the air had finally entrained and disappeared downstream. In the case of the ventilated tip vortices, the cavity would disappear downstream only when about 1.5 to 2 chords depth was reached. A more detailed study of these effects will be made in the future. Figure 10 illustrates the effect of angle of attack on the maximum depth of the surface depression. It can be seen that the foil depth at which the maximum value of d' was measured did not change appreciably with positive angles of attack. In the case of $\alpha = -4^{o}$ the water surface was actually deflected upward. At values of h/c about 0.1 the lower surface of the hydrofoil became ventilated and a relatively thin sheet of water was scooped up by the upper surface. The large negative value of d'/c at small foil submergences represents this sheet of water.

The dependence of the maximum surface depth for various submergence ratios is shown as a funtion of lift coefficient in Fig. 11 and the Froude number in Fig. 12. It is of interest to note from Fig. 12 that the depth-chord ratio is nearly linearly proportional to the Froude number. A theoretical analysis of this depression has been carried out by D. K. Ai and T. Y. Wu, the numerical results of this work will be presented in a future report. It is hoped that this work will explain the salient features of these graphs.

4. Conclusions

From this preliminary experimental study of the water surface contour behind a submerged hydrofoil, the following general conclusions can be made:

1) The surface depression is greatest along the centerline at a distance downstream which is directly related to the Froude number.
2) The maximum depression of the water surface is nearly linearly dependent on lift coefficient and Froude number.

3) The maximum depth increases rapidly with a decrease in foil submergence and attains a maximum value between depth-chord ratio of 0.1 and 0.4, depending on the Froude number.

As the hydrofoil approaches the water surface ventilated tip vortices first appear, followed by superventilation when the foil is at 0.1 to 0.2 chords depth. These air entrainment problems will be studied in more detail in the future. It would be of particular interest to determine the conditions for ventilation of the initial vortex and subsequent superventilation, and the conditions under which the ventilated cavity will disappear again.

REFERENCES

1. Wadlin, K. L., Ramsen, J. A., Vaughan, V. L., Jr.: "The Hydrodynamic Characteristics of Modified Rectangular Flat Plates Having Aspect Ratios of 1.00, 0.25, and 0.125 and Operating Near a Free Water Surface", NACA Report 1246, 1955.

2. Brentjes, J.: "Ventilation Characteristics of a Parabolic and NACA 16-206 Hydrofoil", 16 mm Sound Motion Picture No. 62, Contract Nonr-220(43), Hydrodynamics Laboratory, California Institute of Technology, 1962.

3. Brentjes, J.: "Experimental Force Investigation of a NACA 16-206 Hydrofoil in the California Institute of Technology Free Surface Water Tunnel", Boeing Document D2-11597, Boeing Company, Seattle, Washington, July, 1961.

TABLE I

HYDROFOIL AND STRUT COORDINATES

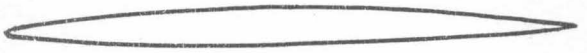

NACA 16-206

NACA 16-006

NACA 16-206				NACA 16-006	
HYDROFOIL				STRUT	
X_u	Y_u	X_ℓ	Y_ℓ	X	Y_u , Y_ℓ
0.	0.	0.	0.	0.	0.
0.0362	0.0225	0.0383	0.01611	0.0281	0.0145
0.0734	0.0326	0.0766	0.0215	0.0563	0.0203
0.1482	0.0467	0.1518	0.0286	0.1125	0.0282
0.2232	0.0582	0.2268	0.0327	0.1683	0.0341
0.2920	0.0674	0.3018	0.0363	0.2250	0.0389
0.4483	0.0822	0.4517	0.0418	0.3375	0.0465
0.5984	0.0938	0.6016	0.0461	0.4500	0.0535
0.8989	0.1104	0.9011	0.0521	0.6750	0.0610
1.1994	0.1199	1.2006	0.0557	0.5000	0.0659
1.5000	0.1231	1.5000	0.0569	1.1250	0.0675
1.8006	0.1196	1.7994	0.0554	1.3500	0.0656
2.1010	0.1082	2.0990	0.0499	1.5750	0.0593
2.4014	0.0868	2.3986	0.0391	1.8000	0.0472
2.7013	0.0532	2.6587	0.0222	2.0250	0.0283
2.8510	0.0307	2.8499	0.0117	2.1375	0.0159
3.000	0.	3.0000	0.	2.2500	0.0014
L. E. RADIUS = 0.00176" SLOPE OF RADIUS THROUGH L. E. = .0824				L. E. RADIUS = .00396	

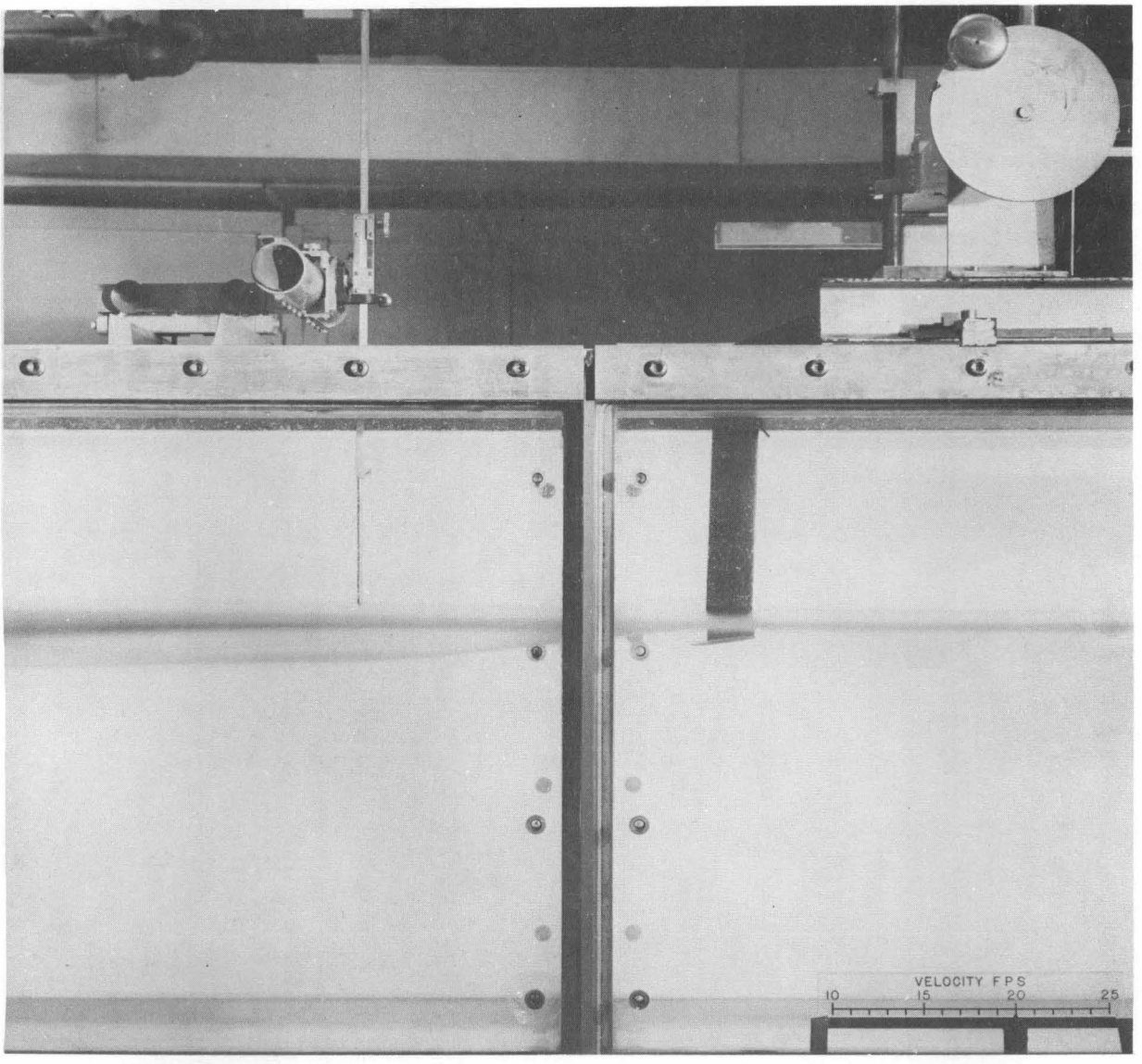

Figure 1. Photograph showing strut-mounted hydrofoil in test section of Free-Surface Water Tunnel. The tunnel velocity is 20 ft. per sec. at an angle of attack of 8^{o} and the submergence ratio (h/c) is 0.25. The following legend identifies the objects in the photograph: (1) Hydrofoil and strut system, (2) Strut support, (3) Depth gage and traversing mechanism, (4) Velocity indicator.

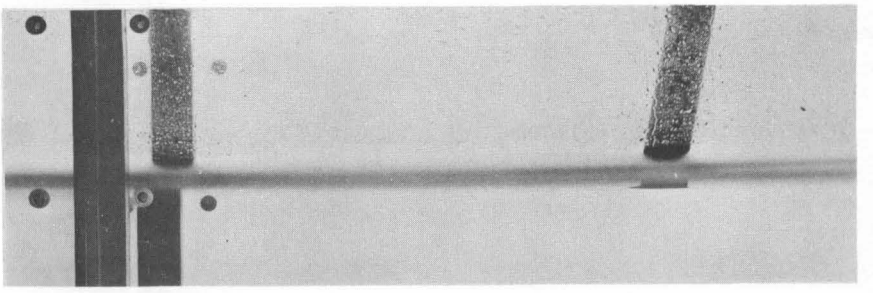

Angle of Attack = 0^{o}, $C_L = 0.015$

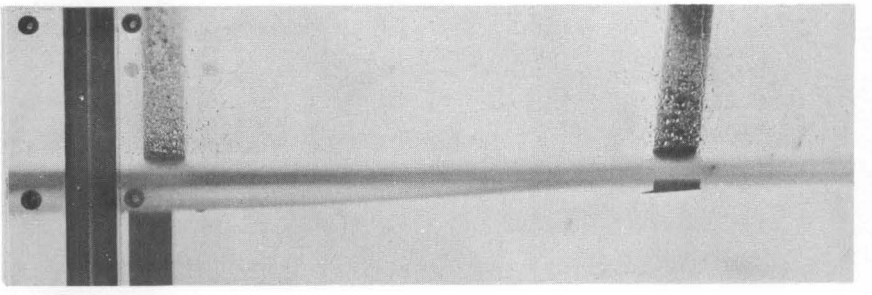

Angle of Attack = 4^{o}, $C_L = 0.120$

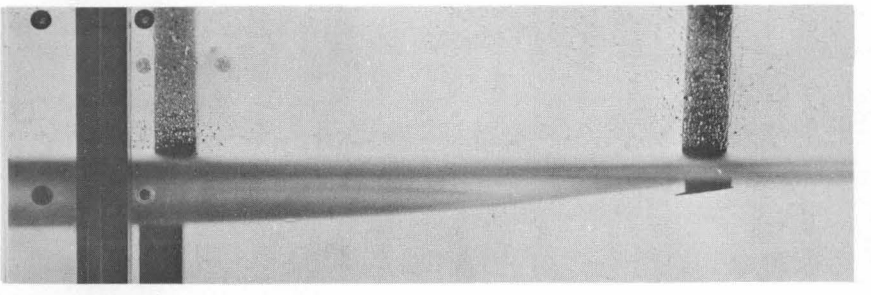

Angle of Attack = 8^{o}, $C_L = 0.232$

Figure 2. Photographs of water surface depression behind hydrofoil at various angles of attack. The ratio of the submergence to the chord is 0.24 and the velocity is 24 ft. per sec.

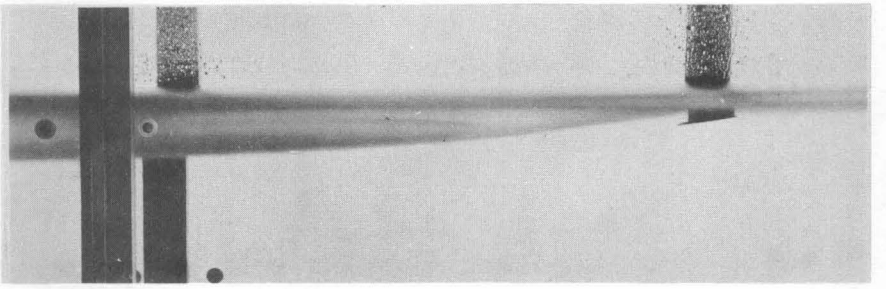

h/c = .236, C_L = 0.230

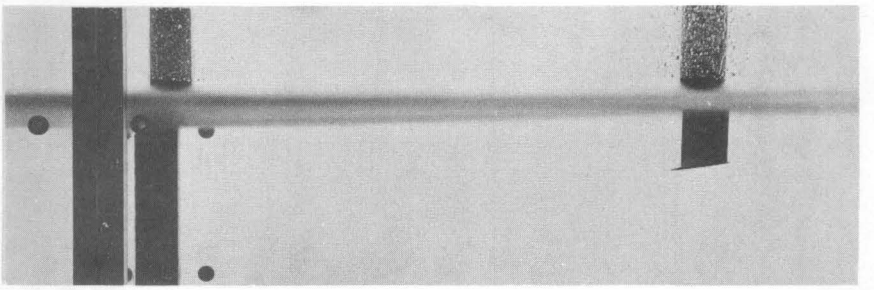

h/c = .98, C_L = 0.323

Figure 3. Effect of submergence on the depression of the water surface. In each case the water velocity is 24.5 ft. per sec. and the angle of attack is 8°.

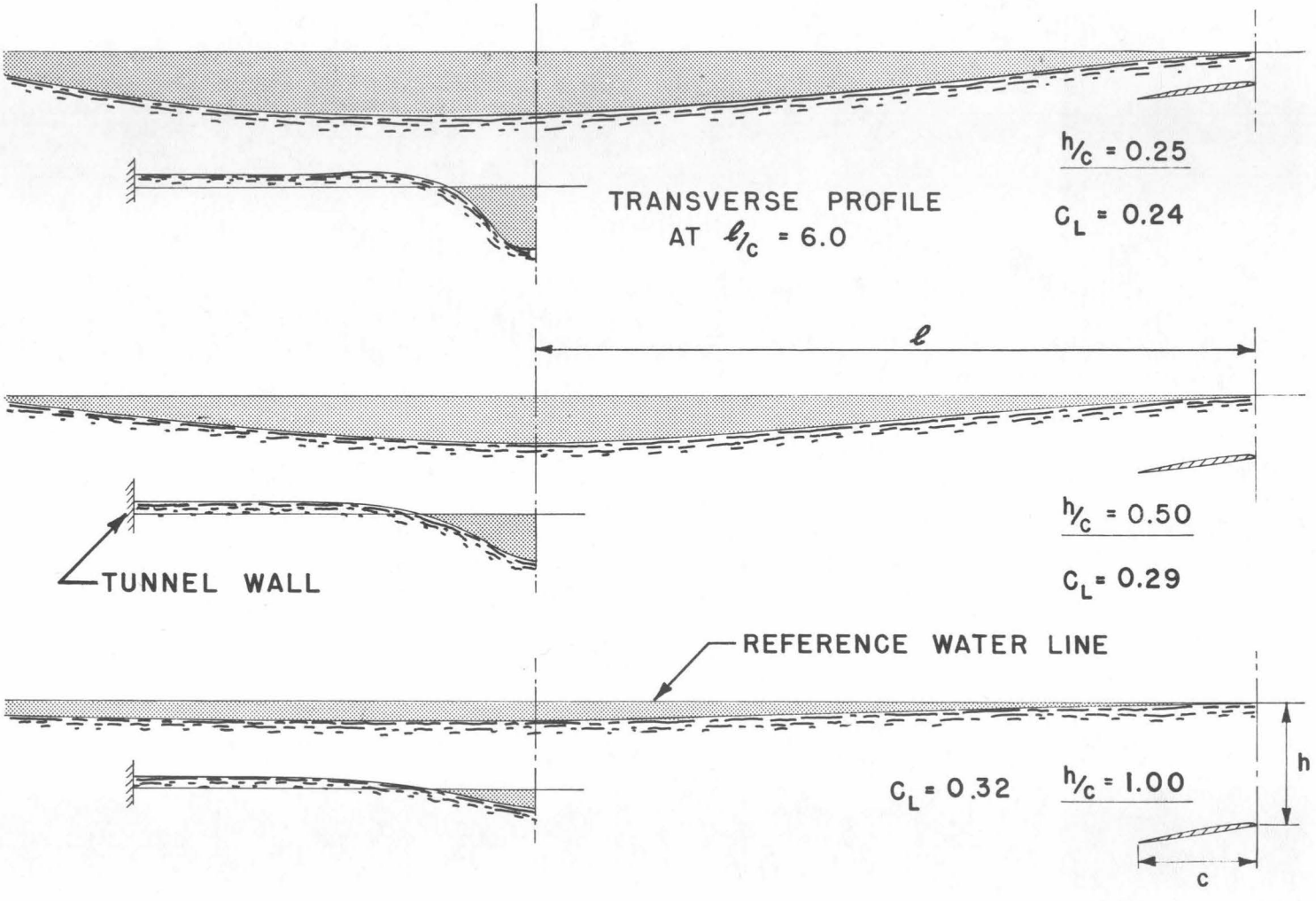

Figure 4. The effect of hydrofoil depth on the water surface profile. The Froude number based on chord is 5.3 and the angle of attack is 8°. For each depth, a longitudinal profile on the centerline of the hydrofoil and a transverse profile six chord lengths downstream are shown. The aspect ratio of the hydrofoil is 4/3.

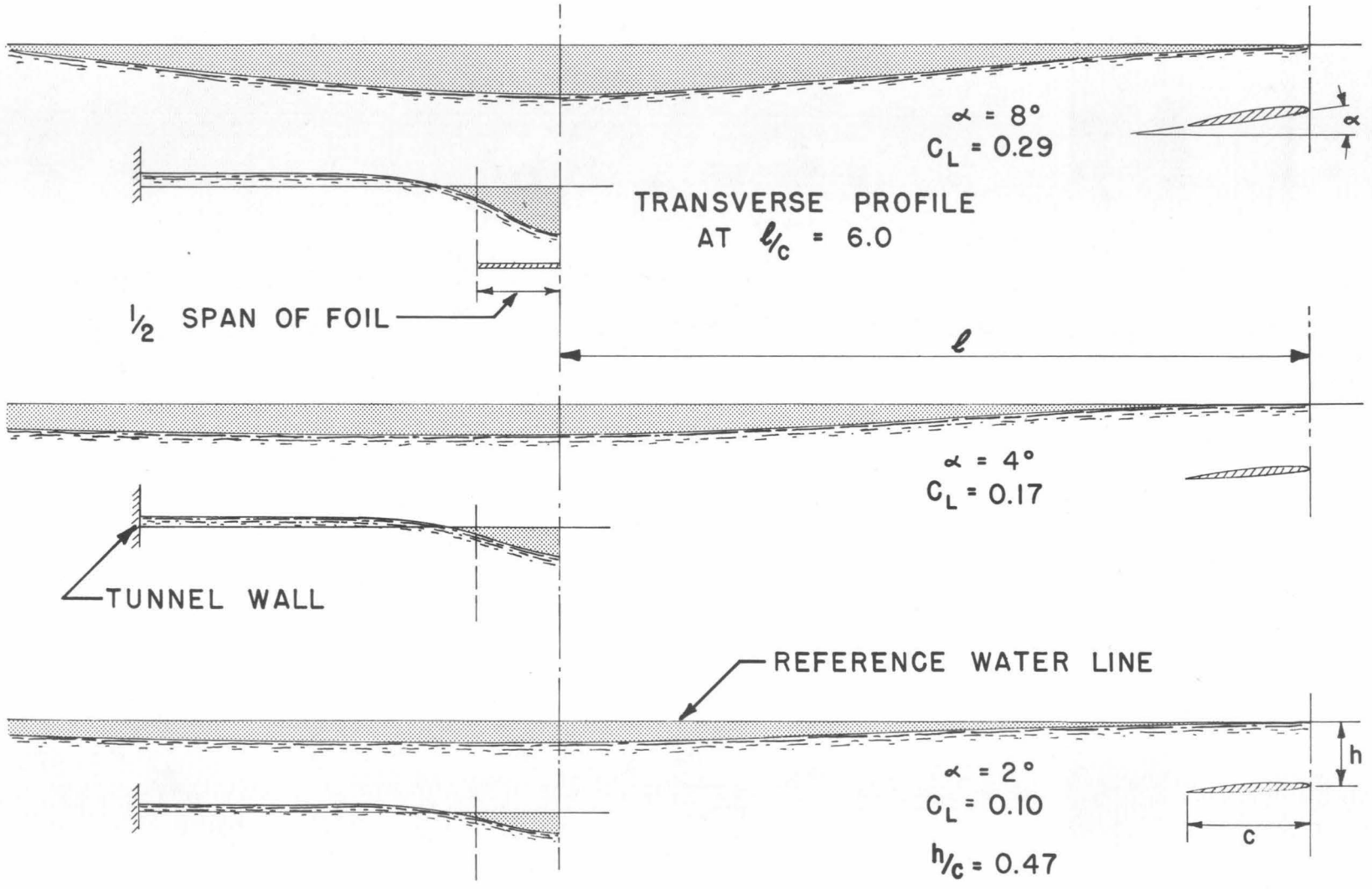

Figure 5. The effect of angle of attack on the water surface profile behind the hydrofoil. The hydrofoil in each case is submerged one-half of its chord length and the Froude number based on chord is 5.3. The aspect ratio of the hydrofoil is 4/3.

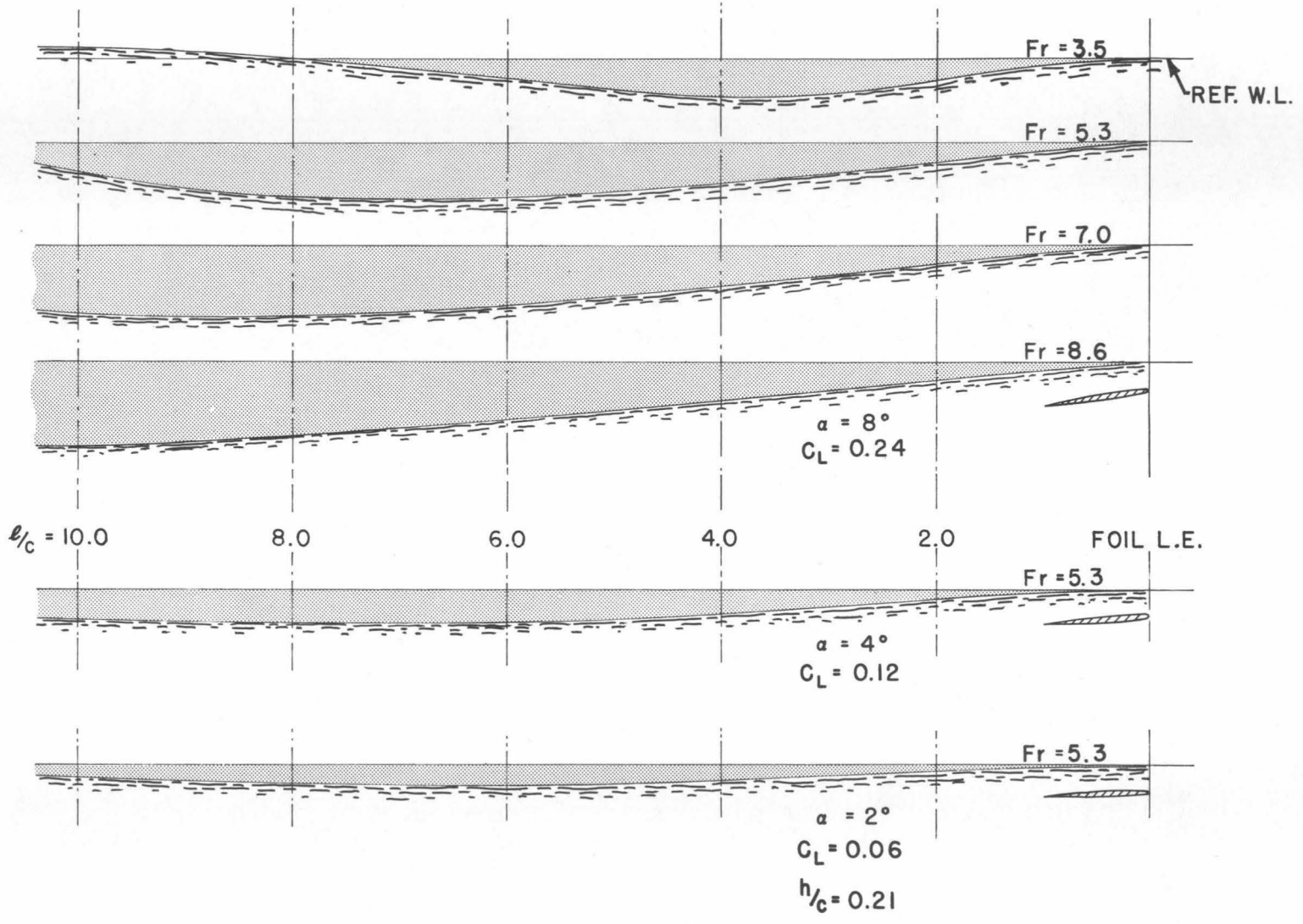

Figure 6. Centerline surface profiles at various angles of attack and Froude numbers at a constant hydrofoil submergence of 0.25 chords.

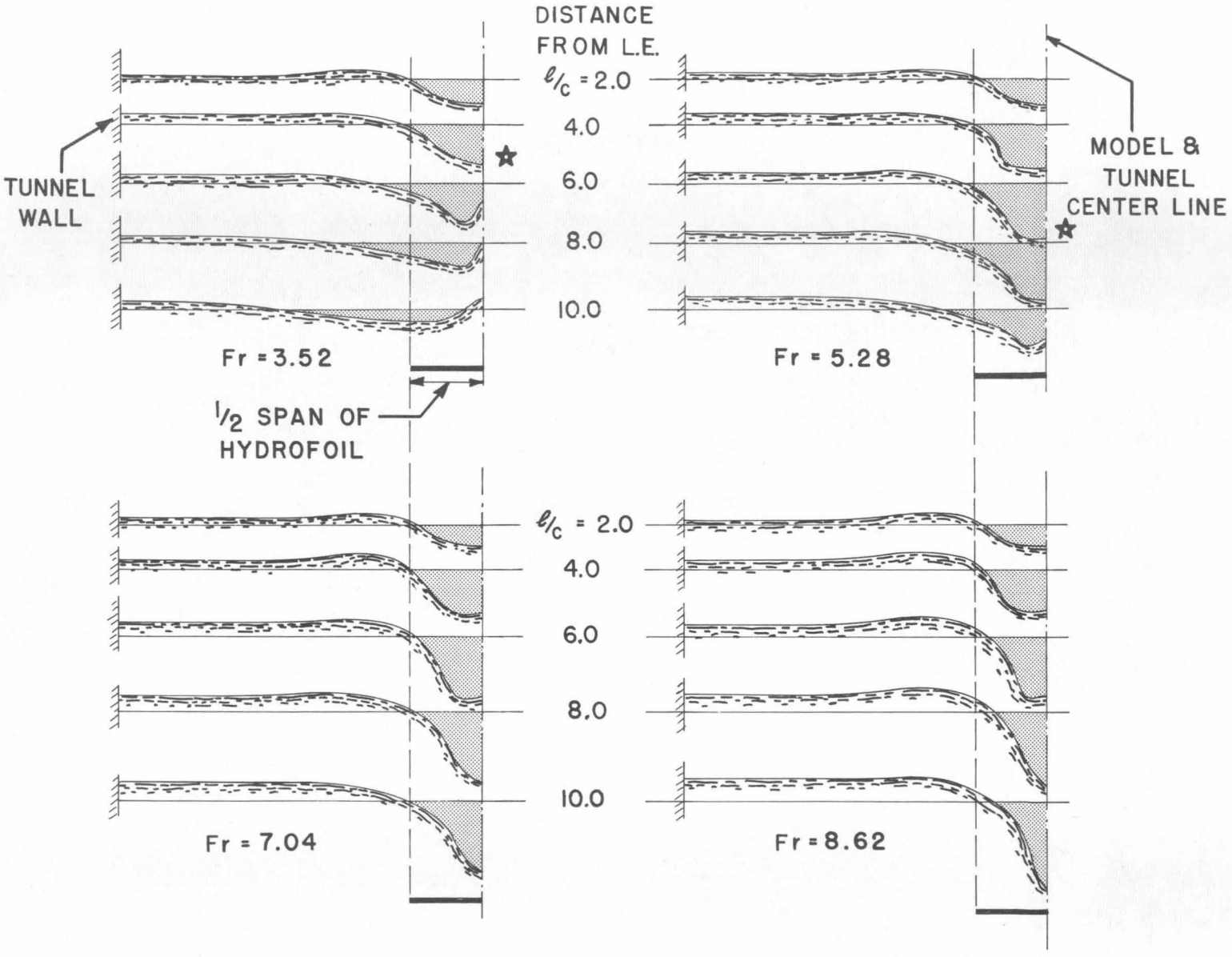

Figure 7. Transverse surface profiles for various Froude numbers at a constant submergence of 0.25 hydrofoil chords and angle of attack of 8°. The "star" on the figure denotes the location of maximum surface depth.

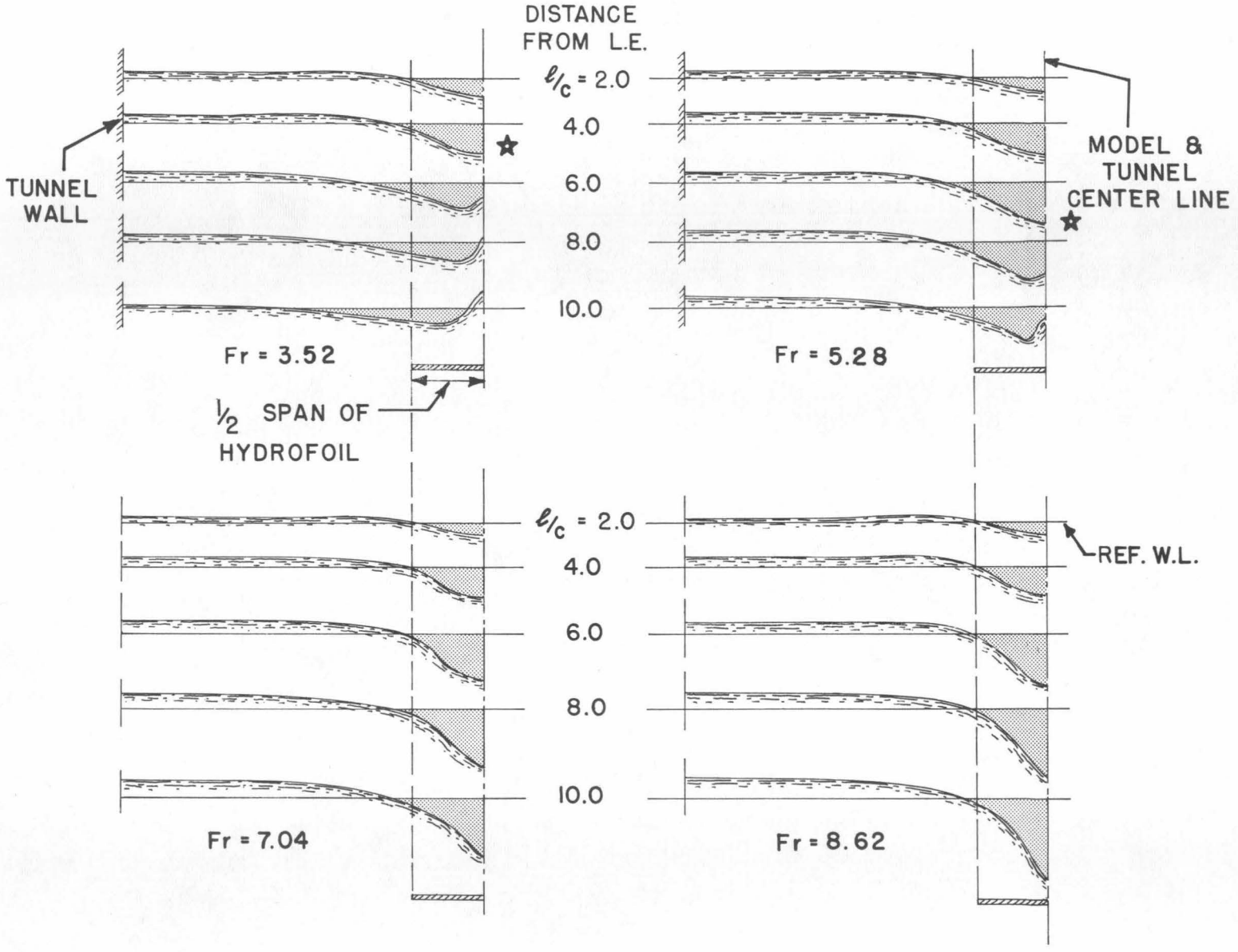

Figure 8. Transverse surface profiles for various Froude numbers at a constant submergence of 0.50 hydrofoil chords at an angle of attack of 8°. The "star" on the figure denotes the location of maximum surface depth.

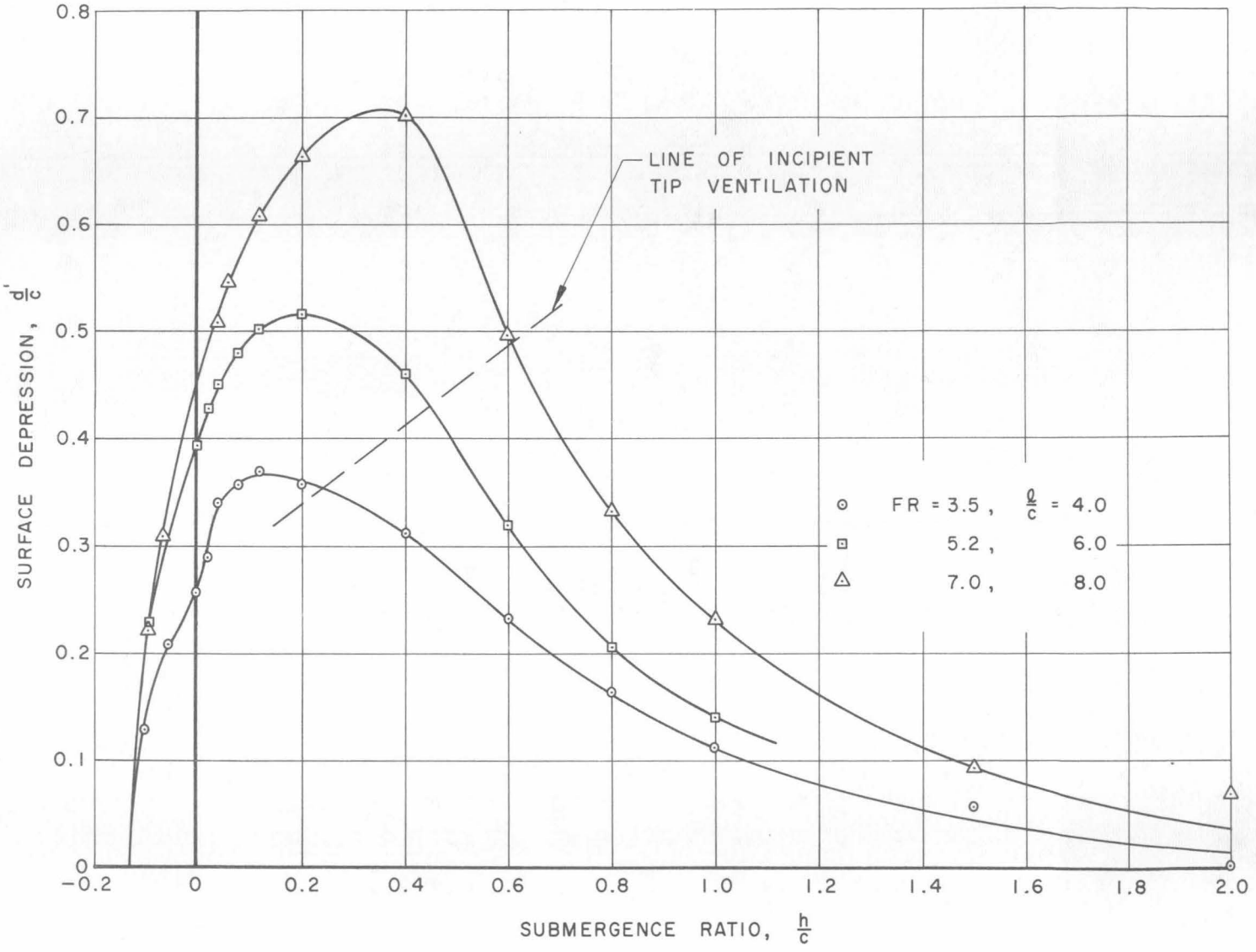

Figure 9. Maximum surface depression behind hydrofoil as a function of submergence and Froude number. The angle of attack is 8^{o} and the aspect ratio of the hydrofoil is 4/3.

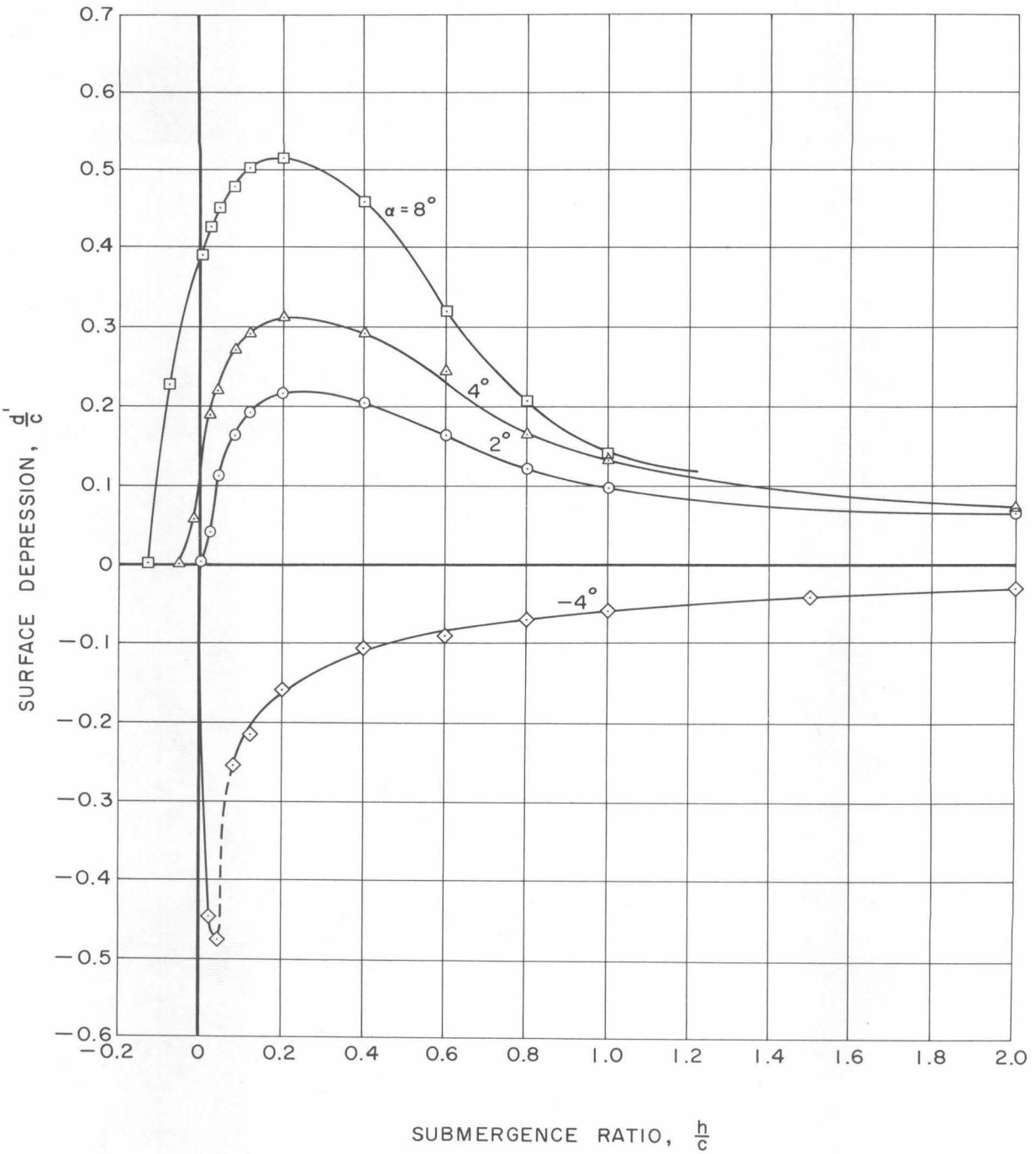

Figure 10. Maximum surface depression behind hydrofoil as a function of submergence ratio and angle of attack. The Froude number is 5.28 (based on chord) for all angles. The aspect ratio of the hydrofoil is 4/3.

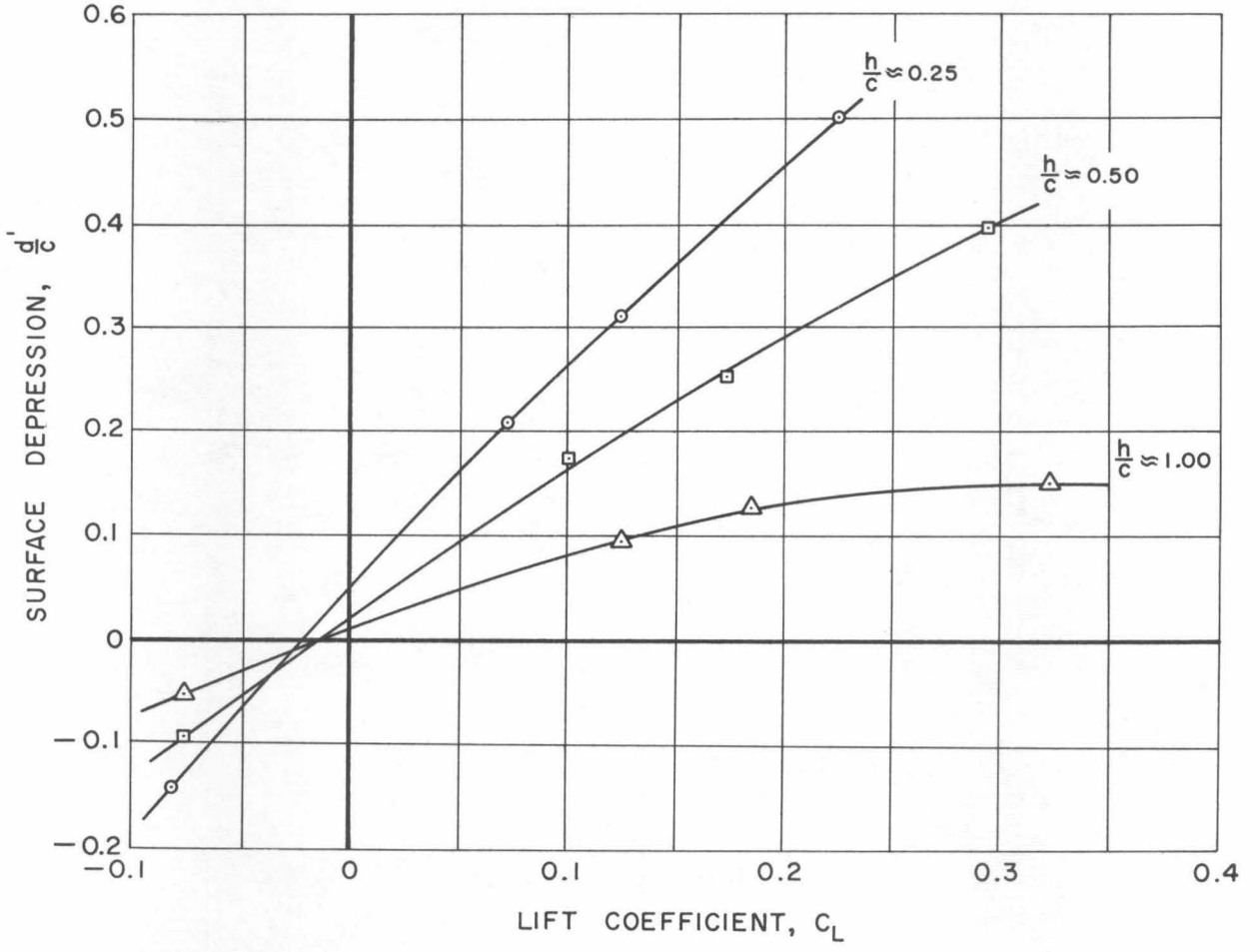

Figure 11. Maximum surface depression as a function of depth and lift coefficient for a Froude number of 5.3 (based on chord). The aspect ratio is 4/3.

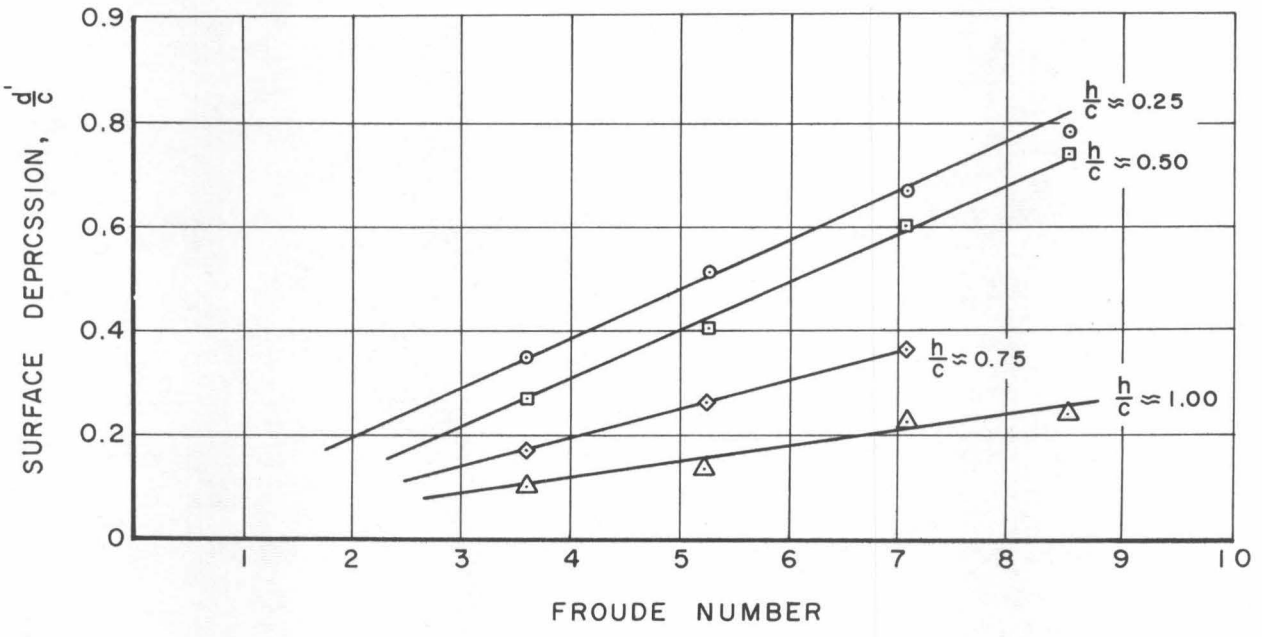

Figure 12. Maximum surface depression as a function of Froude number and submergence ratio.

DISTRIBUTION LIST FOR UNCLASSIFIED TECHNICAL REPORTS
ISSUED UNDER
CONTRACT Nonr-220(43)

(Single copies unless otherwise specified)

Chief of Naval Research
Department of the Navy
Washington 25, D.C.
Attn: Codes 438 (3)
461
463
466

Commanding Officer
Office of Naval Research
Branch Office
495 Summer Street
Boston 10, Massachusetts

Commanding Officer
Office of Naval Research
Branch Office
207 West 24th Street
New York 11, New York

Commanding Officer
Office of Naval Research
Branch Office
1030 East Green Street
Pasadena, California

Commanding Officer
Office of Naval Research
Branch Office
1000 Geary Street
San Francisco 9, California

Commanding Officer
Office of Naval Research
Branch Office
Box 39, Navy No. 100
Fleet Post Office
New York, New York (25)

Director
Naval Research Laboratory
Washington 25, D. C.
Attn: Code 2027 (6)

Chief, Bureau of Naval Weapons
Department of the Navy
Washington 25, D. C.
Attn: Codes RUAW-r
RRRE
RAAD
RAAD-222
DIS-42

Commander
U. S. Naval Ordnance Test Station
China Lake, California
Attn: Code 753

Chief, Bureau of Ships
Department of the Navy
Washington 25, D. C.
Attn: Codes 310
312
335
420
421
440
442
449

Chief, Bureau of Yards and Docks
Department of the Navy
Washington 25, D. C.
Attn: Code D-400

Commanding Officer and Director
David Taylor Model Basin
Washington 7, D. C.
Attn: Codes 108
142
500
513
520
525
526
526A
530
533
580
585
589
591
591A
700

Commander
U.S. Naval Ordnance Test Station
Pasadena Annex
3202 E. Foothill Blvd.
Pasadena 8, California
Attn: Code P-508

Commander
Planning Department
Portsmouth Naval Shipyard
Portsmouth, New Hampshire

Commander
Planning Department
Boston Naval Shipyard
Boston 29, Massachusetts

Commander
Planning Department
Pearl Harbor Naval Shipyard
Navy No. 128, Fleet Post Office
San Francisco, California

Commander
Planning Department
San Francisco Naval Shipyard
San Francisco 24, California

Commander
Planning Department
Mare Island Naval Shipyard
Vallejo, California

Commander
Planning Department
New York Naval Shipyard
Brooklyn 1, New York

Commander
Planning Department
Puget Sound Naval Shipyard
Bremerton, Washington

Commander
Planning Department
Philadelphia Naval Shipyard
U. S. Naval Base
Philadelphia 12, Pennsylvania

Commander
Planning Department
Norfolk Naval Shipyard
Portsmouth, Virginia

Commander
Planning Department
Charleston Naval Shipyard
U. S. Naval Base
Charleston, South Carolina

Commander
Planning Department
Long Beach Naval Shipyard
Long Beach 2, California

Commander
Planning Department
U. S. Naval Weapons Laboratory
Dahlgren, Virginia

Commander
U. S. Naval Ordnance Laboratory
White Oak, Maryland

Dr. A. V. Hershey
Computation and Exterior
Ballistics Laboratory
U. S. Naval Weapons Laboratory
Dahlgren, Virginia

Superintendent
U. S. Naval Academy
Annapolis, Maryland
Attn: Library

Superintendent
U. S. Naval Postgraduate School
Monterey, California

Commandant
U. S. Coast Guard
1300 E. Street, N. W.
Washington, D. C.

Secretary Ship Structure Committee
U. S. Coast Guard Headquarters
1300 E Street, N. W.
Washington, D. C.

Commander
Military Sea Transportation Service
Department of the Navy
Washington 25, D. C.

U. S. Maritime Administration
GAO Building
441 G Street, N. W.
Washington, D. C.
Attn: Division of Ship Design
Division of Research

Superintendent
U. S. Merchant Marine Academy
Kings Point, Long Island, New York
Attn: Capt. L. S. McCready
(Dept. of Engineering)

Commanding Officer and Director
U. S. Navy Mine Defense Laboratory
Panama City, Florida

Commanding Officer
NROTC and Naval Administrative
Massachusetts Institute of Technology
Cambridge 39, Massachusetts

U. S. Army Transportation Research and
Development Command
Fort Eustis, Virginia
Attn: Marine Transport Division

Mr. J. B. Parkinson
National Aeronautics and Space
Administration
1512 H Street, N. W.
Washington 25, D. C.

Director
Langley Research Center
Langley Station
Hampton, Virginia
Attn: Mr. I. E. Garrick
Mr. D. J. Marten

Director Engineering Sciences Division
National Science Foundation
1951 Constitution Avenue, N. W.
Washington 25, D. C.

Director
National Bureau of Standards
Washington 25, D. C.
Attn: Fluid Mechanics Division
(Dr. G. B. Schubauer)
Dr. G. H. Keulegan
Dr. J. M. Franklin

Defense Documentation Center
Cameron Station
Alexandria, Virginia (20)

Office of Technical Services
Department of Commerce
Washington 25, D. C.

California Institute of Technology
Pasadena 4, California
Attn: Professor M. S. Plesset
Professor T. Y. Wu
Professor A. J. Acosta

University of California
Department of Engineering
Los Angeles 24, California
Attn: Dr. A. Powell

Director
Scripps Institute of Oceanography
University of California
La Jolla, California

Professor M. L. Albertson
Department of Civil Engineering
Colorado A and M College
Fort Collins, Colorado

Professor J. E. Cermak
Department of Civil Engineering
Colorado State University
Fort Collins, Colorado

Professor W. R. Sears
Graduate School of Aeronautical Engineering
Cornell University
Ithaca, New York

State University of Iowa
Iowa Institute of Hydraulic Research
Iowa City, Iowa
Attn: Dr. H. Rouse
Dr. L. Landweber

Massachusetts Institute of Technology
Cambridge 39, Massachusetts
Attn: Department of Naval Architecture
and Marine Engineering
Professor A. T. Ippen

Harvard University
Cambridge 38, Massachusetts
Attn: Professor G. Birkhoff
(Dept. of Mathematics)
Professor G. F. Carrier
(Dept. of Mathematics)

University of Michigan
Ann Arbor, Michigan
Attn: Professor R. B. Couch
(Dept. of Naval Architecture)
Professor W. W. Willmarth
(Aero. Engineering Department)

Dr. L. G. Straub, Director
St. Anthony Falls Hydraulic Laboratory
University of Minnesota
Minneapolis 14, Minnesota
Attn: Mr. J. N. Wetzel
Professor B. Silberman

Professor J. J. Foody
Engineering Department
New York State University Maritime College
Fort Schulyer, New York

New York University
Institute of Mathematical Sciences
25 Waverly Place
New York 3, New York
Attn: Professor J. Keller
Professor J. J. Stoker

The Johns Hopkins University
Department of Mechanical Engineering
Baltimore 18, Maryland
Attn: Professor S. Corrsin
Professor O. M. Phillips (2)

Massachusetts Institute of Technology
Department of Naval Architecture and
Marine Engineering
Cambridge 39, Massachusetts
Attn: Professor M. A. Abkowitz, Head

Dr. G. F. Wislicenus
Ordnance Research Laboratory
Pennsylvania State University
University Park, Pennsylvania
Attn: Dr. M. Sevik

Professor R. C. DiPrima
Department of Mathematics
Rensselaer Polytechnic Institute
Troy, New York

Director
Woods Hole Oceanographic Institute
Woods Hole, Massachusetts

Stevens Institute of Technology
Davidson Laboratory
Castle Point Station
Hoboken, New Jersey
Attn: Mr. D. Savitsky
Mr. J. P. Breslin
Mr. C. J. Henry
Mr. S. Tsakonas

Webb Institute of Naval Architecture
Crescent Beach Road
Glen Cove, New York
Attn: Professor E. V. Lewis
Technical Library

Executive Director
Air Force Office of Scientific Research
Washington 25, D. C.
Attn: Mechanics Branch

Commander
Wright Air Development Division
Aircraft Laboratory
Wright-Pattern Air Force Base, Ohio
Attn: Mr. W. Mykytow, Dynamics Branch

Cornell Aeronautical Laboratory
4455 Genesee Street
Buffalo, New York
Attn: Mr. W. Targoff
Mr. R. White

Massachusetts Institute of Technology
Fluid Dynamics Research Laboratory
Cambridge 39, Massachusetts
Attn: Professor H. Ashley
Professor M. Landahl
Professor J. Dugundji

Hamburgische Schiffbau-Versuchsanstalt
Bramfelder Strasse 164
Hamburg 33, Germany
Attn: Dr. H. Schwanecke
Dr. H. W. Lerbs

Institut fur Schiffbau der Universitat Hamburg
Berliner Tor 21
Hamburg 1, Germany
Attn: Prof. G. P. Weinblum,

Transportation Technical Research Institute
1-1057, Mejiro-Cho, Toshima-Ku
Tokyo, Japan

Max-Planck Institut fur Stromungsforschung
Bottingerstrasse 6/8
Gottingen, Germany
Attn: Dr. H. Reichardt

Hydro-og Aerodynamisk Laboratorium
Lyngby, Denmark
Attn: Professor Carl Prohaska

Shipsmodelltanken
Trondheim, Norway
Attn: Professor J. K. Lunde

Versuchsanstalt fur Wasserbau and Schiffbau
Schleuseninsel im Tiergarten
Berlin, Germany
Attn: Dr. S. Schuster, Director
Dr. Grosse

Technische Hogeschool
Institut voor Toegepaste Wiskunde
Julianalaan 132
Delft, Netherlands
Attn: Professor R. Timman

Bureau D'Analyse et de Recherche Appliquees
47 Avenue Victor Bresson
Issy-Les-Moulineaux
Seine, France
Attn: Professor Siestrunck

Netherlands Ship Model Basin
Wageningen, The Netherlands
Attn: Dr. Ir. J. D. vanManen

National Physical Laboratory
Teddington, Middlesex, England
Attn: Mr. A. Silverleaf, Superintendent Ship Division
Head, Aerodynamics Division

Head, Aerodynamics Department
Royal Aircraft Establishment
Farnborough, Hants, England
Attn: Mr. M. O. W. Wolfe

Dr. S. F. Hoerner
148 Busteed Drive
Midland Park, New Jersey

Boeing Airplane Company
Seattle Division
Seattle, Washington
Attn: Mr. M. J. Turner

Electric Boat Division
General Dynamics Corporation
Groton, Connecticut
Attn: Mr. Robert McCandliss

General Applied Sciences Labs., Inc.
Merrick and Stewart Avenues
Westbury, Long Island, New York

Gibbs and Cox, Inc.
21 West Street
New York, New York

Lockheed Aircraft Corporation
Missiles and Space Division
Palo Alto, California
Attn: R. W. Kermeen

Grumman Aircraft Engineering Corp.
Bethpage, Long Island, New York
Attn: Mr. E. Baird
Mr. E. Bower
Mr. W. P. Carl

Midwest Research Institute
425 Volker Blvd.
Kansas City 10, Missouri
Attn: Mr. Zeydel

Director, Department of Mechanical Sciences
Southwest Research Institute
8500 Culebra Road
San Antonio 6, Texas
Attn: Dr. H. N. Abramson
Mr. G. Ransleben
Editor, Applied Mechanics Review

Convair
A Division of General Dynamics
San Diego, California
Attn: Mr. R. H. Oversmith
Mr. H. T. Brooke

Hughes Tool Company
Aircraft Division
Culver City, California
Attn: Mr. M. S. Harned

Hydronautics, Incorporated
Pindell School Road
Howard County
Laurel, Maryland
Attn: Mr. Phillip Eisenberg

Rand Development Corporation
13600 Deise Avenue
Cleveland 10, Ohio
Attn: Dr. A. S. Iberall

U. S. Rubber Company
Research and Development Department
Wayne, New Jersey
Attn: Mr. L. M. White

Technical Research Group, Inc.
Route 110
Melville, New York, 11749
Attn: Mr. Jack Kotik

Mr. C. Wigley
Flat 102
6-9 Charterhouse Square
London, E. C. 1, England

AVCO Corporation
Lycoming Division
1701 K Street, N. W.
Apt. No. 904
Washington, D. C.
Attn: Mr. T. A. Duncan

Mr. J. G. Baker
Baker Manufacturing Company
Evansville, Wisconsin

Curtiss-Wright Corporation Research Division
Turbomachinery Division
Quehanna, Pennsylvania
Attn: Mr. George H. Pedersen

Dr. Blaine R. Parkin
AiResearch Manufacturing Corporation
9851-9951 Sepulveda Boulevard
Los Angeles 45, California

The Boeing Company
Aero-Space Division
Seattle 24, Washington
Attn: Mr. R. E. Bateman
(Internal Mail Station 46-74)

Lockheed Aircraft Corporation
California Division
Hydrodynamics Research
Burbank, California
Attn: Mr. Bill East

National Research Council
Montreal Road
Ottawa 2, Canada
Attn: Mr. E. S. Turner

The Rand Corporation
1700 Main Street
Santa Monica, California
Attn: Technical Library

Stanford University
Department of Civil Engineering
Stanford, California
Attn: Dr. Byrne Perry
Dr. E. Y. Hsu

Dr. Hirsh Cohen
IBM Research Center
P. O. Box 218
Yorktown Heights, New York

Mr. David Wellinger
Hydrofoil Projects
Radio Corporation of America
Burlington, Massachusetts

Food Machinery Corporation
P. O. Box 367
San Jose, California
Attn: Mr. G. Tedrew

Dr. T. R. Goodman
Oceanics, Inc.
Technical Industrial Park
Plainview, Long Island, New York

Professor Brunelle
Department of Aeronautical Engineering
Princeton University
Princeton, New Jersey

Commanding Officer
Office of Naval Research Branch Office
230 N. Michigan Avenue,
Chicago 1, Illinois

University of Colorado
Aerospace Engineering Sciences
Boulder, Colorado
Attn: Prof. M. S. Uberoi

The Pennsylvania State University
Dept. of Aeronautical Engineering
Ordnance Research Laboratory
P. O. Box 30
State College, Pennsylvania
Attn: Professor J. William Holl

Institut fur Schiffbau der Universitat Hamburg
Lammersieth 90
2 Hamburg 33, Germany
Attn: Dr. O. Grim

Technische Hogeschool
Laboratorium voor Scheepsbounkunde
Mekelweg 2, Delft, Netherlands
Attn: Professor Ir. J. Gerritsma